THE JOURNAL OF BIOLOGICAL CHEMISTRY
Vol. 274, No. 32, Issue of August 6, pp. 22170–22175, 1999

Printed in U.S.A.

Phosphoenzyme Conversion of the Sarcoplasmic Reticulum Ca^{2+}-ATPase

MOLECULAR INTERPRETATION OF INFRARED DIFFERENCE SPECTRA*

(Received for publication, March 30, 1999, and in revised form, April 29, 1999)

Andreas Barth‡

From the Institut für Biophysik, Johann Wolfgang Goethe Universität, Theodor Stern Kai 7, Haus 74, D-60590 Frankfurt am Main, Germany

Time-resolved Fourier transform infrared difference spectra of the phosphoenzyme conversion and Ca^{2+} release reaction (Ca_2E_1-P → E_2-P) of the sarcoplasmic reticulum Ca^{2+}-ATPase were recorded at pH 7 and 1 °C in H_2O and ^2H_2O. In the amide I spectral region, the spectra indicate backbone conformational changes preserving conformational changes of the preceding phosphorylation step. β-sheet or turn structures (band at 1685 cm^{-1}) and α-helical structures (band at 1653 cm^{-1}) seem to be involved. Spectra of the model compound EDTA for Ca^{2+} chelation indicate the assignment of bands at 1570, 1554, 1411 and 1399 cm^{-1} to Ca^{2+} chelating Asp and Glu carboxylate groups partially shielded from the aqueous environment. In addition, an E_2-P band at 1638 cm^{-1} has been tentatively assigned to a carboxylate group in a special environment. A Tyr residue seems to be involved in the reaction (band at 1517 cm^{-1} in H_2O and 1515 cm^{-1} in ^2H_2O). A band at 1192 cm^{-1} was shown by isotopic replacement in the γ-phosphate of ATP to originate from the E_2-P phosphate group. This is a clear indication that the immediate environment of the phosphoenzyme phosphate group changes in the conversion reaction, altering phosphate geometry and/or electron distribution.

Muscle relaxation is mediated by the removal of cytosolic Ca^{2+} by the Ca^{2+}-ATPase of the sarcoplasmic reticulum membrane. The ATPase couples active Ca^{2+} transport to the hydrolysis of ATP (1–4) in a reaction cycle that is shown in Scheme 1. In an essential reaction step, ATP reacts with Asp-351 to form a phosphoenzyme intermediate (Ca_2E_1 → Ca_2E_1-P), which then converts from an ADP-sensitive form (Ca_2E_1-P) to an ADP-insensitive form (E_2-P) that is more rapidly hydrolyzed. This phosphoenzyme conversion is associated with Ca^{2+} release toward the sarcoplasmic reticulum lumen against the concentration gradient (1, 3, 5). The structural origin of the change of accessibility of the Ca^{2+} sites and of the essential reduction of Ca^{2+} affinity upon phosphoenzyme conversion Ca_2E_1-P → E_2-P have yet to be elucidated.

The potentially large body of structural information regarding the ATPase reaction cycle provided by infrared spectroscopy has only recently begun to be exploited using the approach of effector molecule-induced infrared difference spectroscopy (6–13). The method uses the release of effector molecules from biologically "silent" photolabile derivatives, termed *caged compounds* (14–17), to generate high quality infrared difference spectra. (The reaction products and infrared difference spectra of caged ATP photolysis and of side reactions have been characterized (18–20).) The absorbance changes seen in these difference spectra give evidence for conformational changes of the polypeptide backbone and for alterations to the environment of amino acid side chains that take place in the reaction investigated.

Spectra of the phosphoenzyme conversion reaction in the 1800 to 1000 cm^{-1} spectral range have previously been described (8) and in that work were calculated by subtracting two difference spectra obtained with two different types of samples; a normalized difference spectrum of the Ca_2E_1 → Ca_2E_1-P reaction was subtracted from a normalized difference spectrum of the Ca_2E_1 → E_2-P reaction. The use of two different samples in the subtraction and the normalization to identical protein content limit the reliability of these spectra and make it desirable to obtain the phosphoenzyme conversion spectrum more directly. This is possible using time-resolved rapid scan Fourier transform infrared (FTIR)[1] spectroscopy (10). Using this approach, we present here the spectra of the phosphoenzyme conversion reaction obtained in H_2O and ^2H_2O after the release of unlabeled ATP or [γ-$^{18}O_3$]ATP. In particular, bands of the putative Ca^{2+} chelating carboxylate groups and of the phosphoenzyme phosphate group are discussed.

MATERIALS AND METHODS

Sample Preparation—Samples for time-resolved infrared spectroscopy of the Ca_2E_1 P → E_2-P reaction were prepared as described previously (8, 10) by removal of free water from a sarcoplasmic reticulum suspension equilibrated in H_2O or ^2H_2O buffer. Samples were immediately rehydrated with H_2O or ^2H_2O with or without 20% Me_2SO. This method resulted in active ATPase samples (6). Approximate concentrations were 0.7 mM ATPase, 300 mM imidazole, pH 7.0, 1 mM $CaCl_2$, 20 mM glutathione, 20 mM caged ATP, 0.5 mg/ml A23187, 2 mg/ml adenylate kinase, and 20% Me_2SO in approximately 1 μl of sample volume. Approximately 2–3 mM ATP was released per flash. Caged [γ-$^{18}O_3$]ATP at 91% isotopic enrichment per oxygen atom was a gift of M. R. Webb and J. E. T. Corrie (National Institute for Medical Research, London).

FTIR Measurements—Time-resolved FTIR measurements of the Ca_2E_1-P → E_2-P reaction were performed at 1 °C with a modified Bruker IFS 66 spectrometer as described previously (10). Difference spectra for the reaction were obtained by subtracting a spectrum representing predominantly Ca_2E_1-P, and to a small extent E_2-P (recorded 3.3–11 s after photolysis of caged ATP in H_2O or after 11–19 s in ^2H_2O), from a spectrum representing E_2-P (recorded after 88 and 146 s in H_2O and ^2H_2O, respectively). The resulting spectrum was normalized as described (10) to the full amplitude of the absorbance changes associated with the phosphoenzyme conversion reaction.

* The costs of publication of this article were defrayed in part by the payment of page charges. This article must therefore be hereby marked "*advertisement*" in accordance with 18 U.S.C. Section 1734 solely to indicate this fact.

‡ To whom correspondence should be addressed. Tel.: 49-69-6301-6087; Fax: 49-69-6301-5838; E-mail: barth@biophysik.uni-frankfurt.de.

[1] The abbreviations used are: FTIR, Fourier transform infrared; Ca^{2+}-ATPase, Ca^{2+} transporting ATPase (EC 3.6.1.38); caged ATP, P^3-1-(2-nitrophenyl)ethyladenosine 5′-triphosphate; Ca_2E_1-P, ADP-sensitive phosphoenzyme; E_2-P, ADP-insensitive phosphoenzyme; ν_s, symmetric stretching vibration; ν_{as}, antisymmetric stretching vibration.

As the difference spectra were obtained directly from the time-resolved measurements, a normalization of spectra to an identical protein concentration is in principle not necessary. However, for a better comparison of samples in H_2O and ^2H_2O and to prevent the possible predominance of individual samples with high protein content in the averaged spectra, spectra were normalized to an identical protein concentration before averaging, as described (21).

Absorbance spectra in H_2O and ^2H_2O of the model compound for Ca^{2+} release EDTA were recorded with and without Ca^{2+} at 20 °C and pH 12.8. Small variations in the path length between different samples were corrected by normalizing the water absorption of every sample to a single water spectrum that served as a standard for the path length. Sample concentrations were 84 mM.

Band-narrowing Procedures—Apart from second-derivative spectra, the following procedure was applied. The original spectrum was smoothed over 24 cm^{-1} and multiplied by 0.95. This spectrum was then subtracted from the original spectrum, which eliminates broad features of the original spectrum. The resulting spectrum is dominated by the fine-structure in the original spectrum, and thus we term the method "fine-structure enhancement" in the following text. When tested with protein absorbance spectra, this method gives results similar to Fourier self-deconvolution (data not shown). For a clearer presentation, fine-structure enhanced spectra were multiplied by 10 and second-derivative spectra by −15.

To assess whether peaks in the fine-structure enhanced spectra correspond to "true" component bands or are the result of artifacts in the band-narrowing procedure (see Fig. 3), the original difference spectra were fitted, and the resulting fit was fine-structure enhanced and compared with the fine-structure enhanced original spectra (data not shown). Interestingly, it was found that the spectral region of 1700–1670 cm^{-1} can accurately be fitted by only three bands at 1693 (−), 1686 (−), and 1670 cm^{-1} (+) despite the plateau at 1678/1676 cm^{-1} in the fine-structure enhanced H_2O spectrum (*solid line* in Fig. 3*B*). It is not necessary to introduce an additional band in the fitting model to reproduce that plateau.

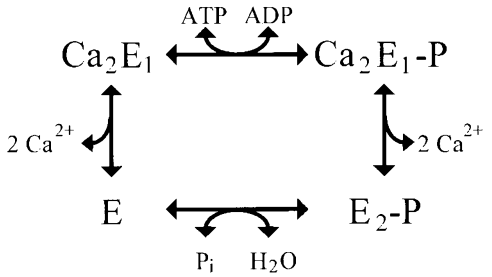

SCHEME 1.

RESULTS AND DISCUSSION

Model Spectra of Ca^{2+} Release—From site-directed mutagenesis studies it is thought that Glu-309, Glu-771, and Asp-800 form part of the high affinity Ca^{2+} binding sites of Ca_2E_1 and Ca_2E_1-P (4). Thus, we studied the effect of Ca^{2+} binding on the infrared spectrum of carboxylate groups using the Ca^{2+} chelator EDTA.

Fig. 1*A* shows absorbance spectra in ^2H_2O of free EDTA (*solid line*) and of the EDTA complex with Ca^{2+} (*dotted line*). The bands near 1590 and 1410 cm^{-1} can be assigned to the COO^- antisymmetric stretching vibration (ν_{as}) and the symmetric stretching vibration (ν_s), respectively. The shoulder at 1612 cm^{-1} indicates some heterogeneity of the COO^- groups, resulting from a small proportion of EDTA with protonated nitrogen atoms (22, 23). Upon Ca^{2+} release there is a downshift of 4–8 cm^{-1} for both of the main bands (at 1590 and 1414 cm^{-1}), which translates in the difference spectrum of Ca^{2+} release (absorbance of free EDTA minus absorbance of the Ca^{2+} complex) into the two minimum/maximum features at 1590/1568 and 1418/1400 cm^{-1}.

When ^2H_2O is replaced by H_2O, the bands of the antisymmetric stretching vibration are downshifted by 6–8 cm^{-1} for free EDTA and for the complex (data not shown). The band of the symmetric stretching vibration is less sensitive and shifts

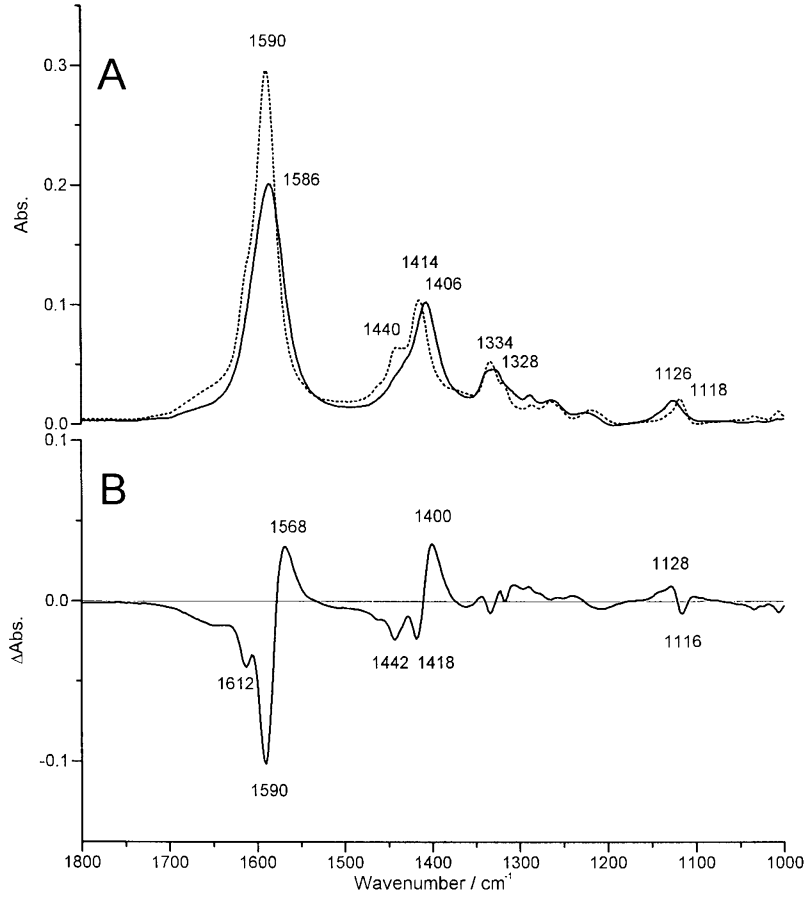

FIG. 1. **Model spectra for Ca^{2+} release from carboxylate groups.** *A*, absorbance spectra in ^2H_2O of EDTA (*solid line*) and the Ca^{2+} complex of EDTA (*dotted line*). *B*, Ca^{2+} release spectrum: absorbance of EDTA minus absorbance of the Ca^{2+} complex of EDTA.

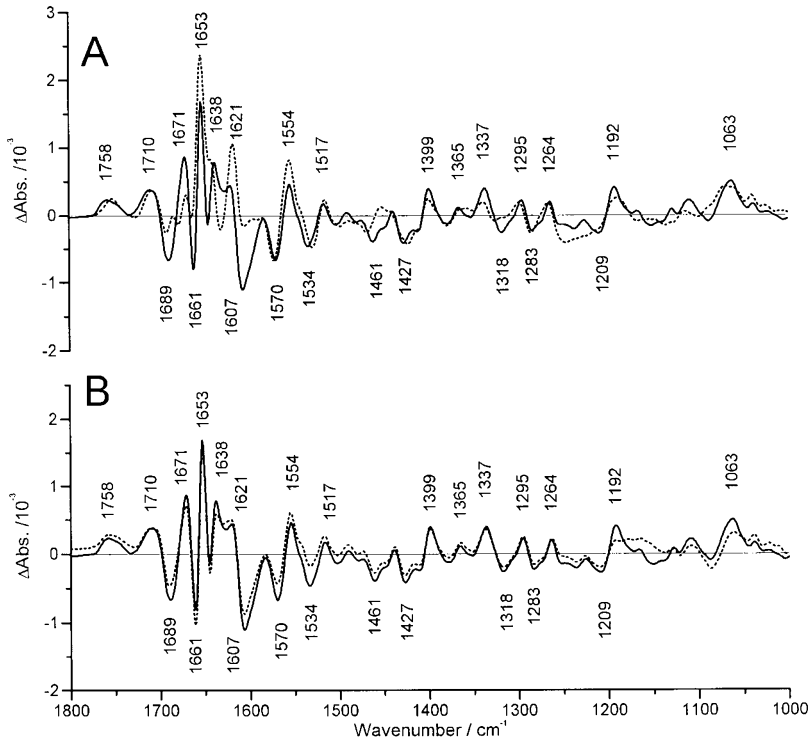

FIG. 2. **Spectra of phosphoenzyme conversion and Ca^{2+} release at pH 7.0 and 1 °C.** The *labels* refer to the *solid line* spectra. *A*, *full line,* H_2O; *dotted line*, ^2H_2O. *B*, spectra in H_2O after the release of unlabeled ATP (*solid line*) and [γ-$^{18}O_3$]ATP (*dotted line*) from caged ATP.

downwards only for free EDTA (by 2 cm^{-1}). A similar behavior has been observed for sodium acetate (24) and for Asp and Glu (25, 26).

Thus, the model spectra have identified marker band pairs for Ca^{2+} release from carboxylate groups near 1575 and 1410 cm^{-1}. The former is expected to be sensitive to $H_2O \rightarrow {}^2H_2O$ replacement with a higher frequency in ^2H_2O.

The Phosphoenzyme Conversion Spectrum—Fig. 2*A* shows the difference spectrum of the phosphoenzyme conversion and Ca^{2+} release reaction, Ca_2E_1-P $\rightarrow E_2$-P (*solid line*), and the respective spectrum in ^2H_2O buffer (*dashed line*). Positive bands are characteristic for E_2-P, negative bands for Ca_2E_1-P. Fig. 3*A* shows the same spectra on an expanded scale.

Ca^{2+} Release from Carboxylate Groups—In the phosphoenzyme conversion spectrum, similar band profiles are observed as in the model difference spectrum for Ca^{2+} release (Fig. 1*B*) at 1570/1554 and 1411/1399 cm^{-1} (numbers for H_2O). The slight upshift upon $H_2O \rightarrow {}^2H_2O$ exchange characteristic for the ν_{as} vibration of carboxylate groups (see above) is also notable (1570 $\rightarrow$ 1572 cm^{-1}, 1554 $\rightarrow$ 1555 cm^{-1}) and is best seen in Fig. 3*A*. However, the shift is less than that observed above for completely exposed carboxylate groups. The lower wavenumber of the 1570/1554 cm^{-1} band pair as compared with the model spectra (1586/1556 cm^{-1} in H_2O and 1590/1568 cm^{-1} in ^2H_2O) is expected because the $\nu_{as}(COO^-)$ band position of free Asp and Glu residues (25, 26) is 2–4 cm^{-1} (Asp) and 18 cm^{-1} (Glu) lower than that of EDTA (in H_2O and ^2H_2O). These observations support and substantiate the tentative assignment of the band pairs at 1570/1554 and 1411/1399 cm^{-1} (numbers for H_2O) to Ca^{2+} chelating residues of the ATPase (8). The relatively small shift observed for the 1570/1554 cm^{-1} band pair in ^2H_2O may indicate that these groups are not completely exposed to water.

The band at 1638 cm^{-1} also shows the upshift characteristic of a $\nu_{as}(COO^-)$ band upon $H_2O \rightarrow {}^2H_2O$ replacement (best seen in Fig. 3*A*). Other bands absorbing in that region, *i.e.* the amide I mode of β-sheet structures, and side chain modes of His, Arg, and Lys should either show downshifts of about 10 cm^{-1} (backbone and His) (26–30), 50 cm^{-1} (Arg) (25, 26), and 400 cm^{-1} (Lys) (31) or should remain unchanged if the respective groups are inaccessible to $^1H \rightarrow {}^2H$ exchange. The position of the 1638 cm^{-1} band is rather unusual for a ν_{as} band of a COO^- group, which absorbs for model compounds in aqueous solution at 1574 cm^{-1} (Asp) or at 1560 cm^{-1} (Glu) (25). However, a strong salt bridge or hydrogen bond to one of the oxygens of a carboxylate group could shift the band well above 1600 cm^{-1} (24, 32), and a reasonable scenario for the band at 1638 cm^{-1} could be that the parting Ca^{2+} is replaced by a strong hydrogen bond donor or a positive charge.

Bands at 1758 and 1710 cm^{-1} have tentatively been assigned to the protonation of at least two chelating carboxylate groups (33), which is in line with the small downshift observed upon $H_2O \rightarrow {}^2H_2O$ replacement.

Protein Backbone: the Amide I Region—The largest absorbance changes (up to 0.5% of the total protein absorbance) are observed in the amide I region of the spectrum (1700–1610 cm^{-1}) as are the strongest effects of protein deuteration. In this region, the amide I mode of the polypeptide backbone as well as the side chains of Asn, Gln, Arg, $HisH^+$, and Lys absorb strongly (25, 26, 30). In the lower wavenumber part of that region, Asp and Glu COO^- groups with strong interactions may contribute as discussed above.

Large downshifts ($\geq$30 cm^{-1}) of bands upon $H_2O \rightarrow {}^2H_2O$ replacement are characteristic for the side chain absorptions of Asn, Gln, Lys, and Arg, as are small upshifts as discussed above for COO^- bands and downshifts of up to 10 cm^{-1} for amide I and $HisH^+$ bands. No band shifts are expected for groups that are located in parts of the protein that are not accessible to deuteration.

The large number of alterations in this spectral region, when H_2O is replaced by ^2H_2O, makes it difficult to arrive at a unique explanation for the band shifts, and additional experiments as well as data processing were necessary, as described below.

The recording of spectra as soon as possible after $H_2O \rightarrow {}^2H_2O$ replacement (30 min to 1 h at 1 °C) shows that most of the observed effects take place in protein regions readily accessible to deuteration. The spectrum shortly after deuteration (data not shown) is very similar to the one after prolonged incuba-

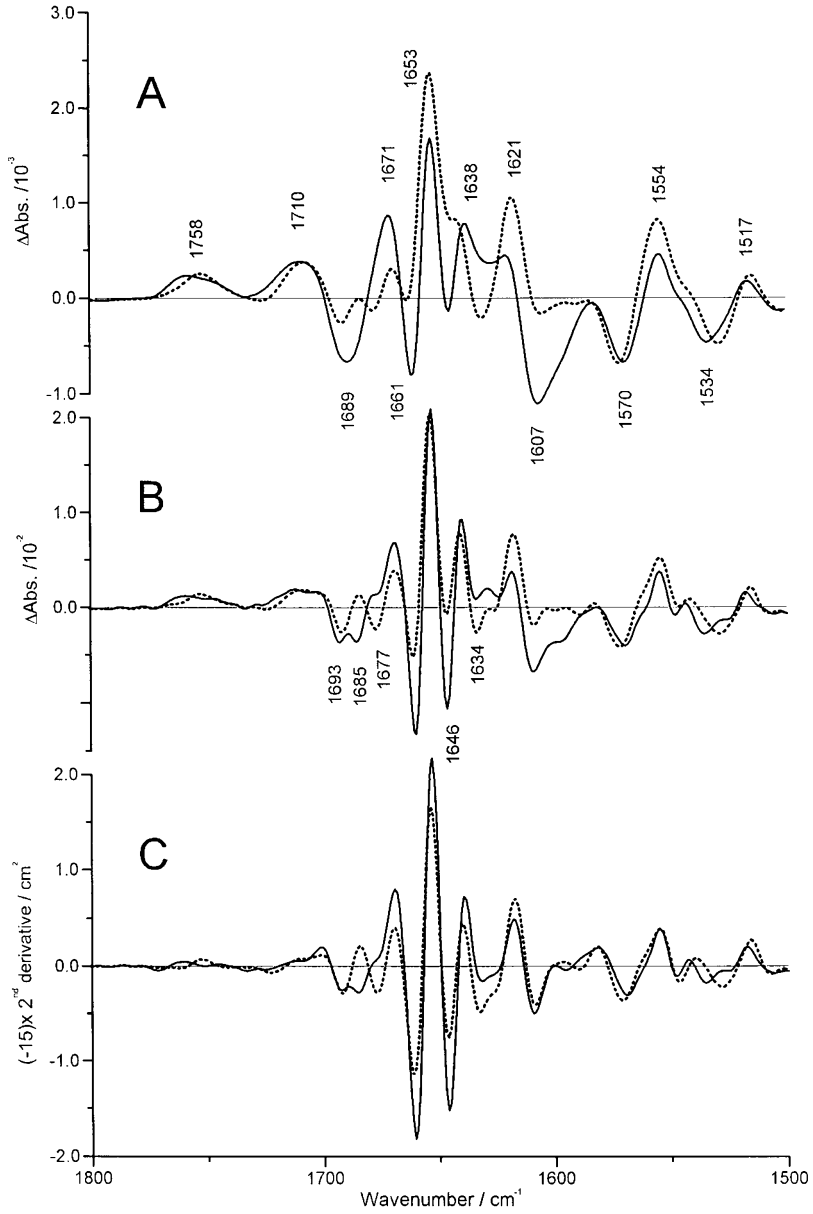

FIG. 3. **Phosphoenzyme conversion spectra processed with band-narrowing techniques.** *A*, original spectra: *solid line*, H_2O; *dotted line*, ^2H_2O. The *labels* refer to the solid line spectrum. *B*, fine structure-enhanced spectra multiplied by 10 (see "Materials and Methods"): *solid line*, H_2O; *dotted line*, ^2H_2O. The *labels* refer to the closest peak. *C*, second derivative spectra multiplied by −15: *full line*, H_2O; *dotted line*, ^2H_2O.

tion. The only clear exception is the minimum at ~1630 cm^{-1} that develops over a few hours of incubation. This position is characteristic of amide I modes of β-sheet structures and of the C=O group of deuterated Asn or Gln residues (26).

Band-narrowing procedures (see "Materials and Methods") were applied to identify band shifts upon $^1H \rightarrow {}^2H$ exchange. Fig. 3*A* shows the original difference spectra and Fig. 3, *B* and *C*, the resulting spectra after band narrowing. These reveal essentially the same peak positions in H_2O and ^2H_2O (see Fig. 3, *B* and *C*), with one exception. The negative band at 1689 cm^{-1} in the unprocessed original H_2O spectrum (*solid line* in Fig. 3*A*) is composed of at least two bands, giving minima in the processed spectrum at 1693 and 1685 cm^{-1} (*solid line* in Fig. 3, *B* and *C*). The highest wavenumber component of the negative band seems to be nearly unaffected by protein deuteration and is observed in ^2H_2O at 1692 cm^{-1}. It could be caused by a conformational change of β-sheet or turn structures or an Asn, Gln, or Arg side chain that is located in the core of the protein and is inaccessible to deuteration.

The other component of the 1689 cm^{-1} band seems to shift from its position in the processed spectrum (Fig. 3*B*) at 1685 (H_2O) to 1677 cm^{-1} (^2H_2O) and to cancel part of the adjacent positive band observed at 1671 cm^{-1} in H_2O (Fig. 3*A*). This shift is characteristic of amide I modes of the polypeptide backbone, and the position then indicates a conformational change of β-sheet or turn structures. These structures are predicted to occur only in the extramembraneous domains of the protein (34, 35), and thus the observed conformational change is likely to take place in these protein domains.

As the positions of the other bands in the amide I region are hardly affected by deuteration, the isotope effects are the result either of intensity changes or of bands that are not evident after applying the band-narrowing procedures because they are broader than the ones detected. Narrow bands tend to dominate the processed spectra.

The bands hardly affected by $^1H \rightarrow {}^2H$ exchange are found at 1653, 1638, 1621, and 1607 cm^{-1}. A band at 1653 cm^{-1} is often observed for α-helical structures and is often hardly affected by $H_2O \rightarrow {}^2H_2O$ replacement as observed here. The band at 1638 cm^{-1}, which shifts slightly upward, was tentatively assigned above to a COO^- group. The bands at 1621 and 1607 cm^{-1} seem to retain their position in ^2H_2O with a possible overlap of additional bands in H_2O or ^2H_2O. The band at 1621 cm^{-1} may be assigned to a β-sheet structure or to the imide group of a Pro

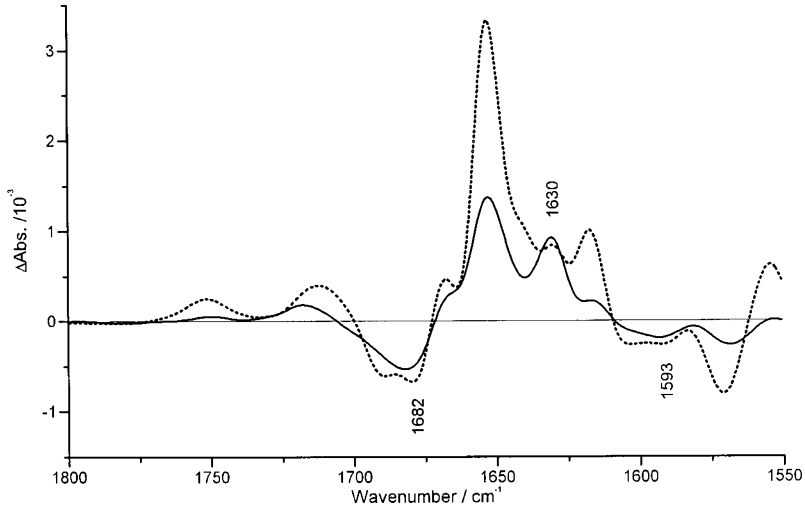

FIG. 4. **Difference spectra of the Ca_2E_1·ATP → Ca_2E_1-P (*solid line*) and the Ca_2E_1·ATP → E_2-P (*dotted line*) reaction at pH 7 and 1 °C.**

residue in a helical or unordered conformation. The imide band is found approximately 20 cm^{-1} lower than an amide band (36). Thus, the band at 1607 cm^{-1}, the position of which seems to be too low for an amide I band, could also be caused by a Pro imide group. Interestingly, there are three Pro residues in the putative Ca^{2+} binding transmembrane helices M4 and M6, mutation of which affects Ca^{2+} affinity and phosphoenzyme conversion (4). Alternatively, both bands may be caused by COO^- side chain groups not interacting with bulk water. This assumption relies on the fact that the bands do not show the upshift upon $H_2O \rightarrow {}^2H_2O$ replacement characteristic for carboxylate groups in water.

Protein Backbone: the Amide II Region—None of the three bands in the amide II region (1570–1530 cm^{-1}) shows the strong sensitivity toward $^1H \rightarrow {}^2H$ exchange expected for the amide II mode of the protein backbone. The amide II mode of backbone elements accessible to deuteration therefore does not seem to be affected by phosphoenzyme conversion and Ca^{2+} release. Two of the bands (at 1570 and 1554 cm^{-1}) have been tentatively attributed above to the ν_{as} vibration of COO^- groups.

Protein Backbone: the Amide III Region—The amide III mode absorbs between 1400 and 1200 cm^{-1} and is sensitive to deuteration (37). This property is observed in the spectra for the bands at 1337 and 1318 cm^{-1} (see Fig. 2*A*), which therefore might be attributed to amide III modes. The position of these bands is characteristic for turn structures (37), and they are probably related to the amide I band at 1687 cm^{-1}, which has tentatively been assigned to turn or β-sheet structures. Alternatively, the bands at 1337 and 1318 cm^{-1} may be caused by the δ(COH) mode of Ser, Asp, or Glu with a weakly bonded OH group.

Side Chain Modes Other than Carboxyl Modes—As mentioned above, bands of the side chains of Asn, Gln, Arg, and Lys in the amide I region show relatively large shifts upon deuteration. The extinction coefficient of the former three residues is relatively high (25, 26), whereas that of Lys is smaller. Thus, Lys bands may be masked by stronger bands. The $HisH^+$ mode near 1631 cm^{-1} (30) shows a 10 cm^{-1} downshift in ^2H_2O (26) and absorbs relatively strongly in H_2O (30). These characteristic shifts have not been observed in the spectra, and thus there is no clear evidence for the participation of Asn, Gln, Arg, and $HisH^+$ in the phosphoenzyme conversion and Ca^{2+} release reaction. This statement holds only for those residues that are accessible to $^1H \rightarrow {}^2H$ exchange, which should include residues in the ATP binding site, the catalytic site, and at least part of the Ca^{2+} binding sites, because several bands that were tentatively assigned to the Ca^{2+} binding sites show an effect upon $H_2O \rightarrow {}^2H_2O$ replacement (see above).

The position of the band at 1517 cm^{-1} and its slight downshift of 2 cm^{-1} in ^2H_2O is characteristic for a ring mode of protonated Tyr (25, 26, 30). Also, the band pairs at 1283 and 1264 cm^{-1} may be attributed to the ν(C-O) mode of Tyr but also to a Trp mode, which is observed for indole at 1276 cm^{-1} (38, 39). It has been suggested that Tyr-763 is involved in the cytoplasmic gate to the Ca^{2+} binding sites (4). The very small band at 1365 cm^{-1} might be caused by a $\delta_s(CH_3)$ mode of aliphatic side chains.

Absorption of the Phosphate Group—Fig. 2*B* shows a comparison between the conversion spectrum obtained with unlabeled ATP and that obtained with [γ-$^{18}O_3$]ATP. With the heavier isotope, phosphate bands are expected to be downshifted, thereby enabling the identification in the spectrum of alterations to the phosphate group. As the γ-phosphate is transferred to Asp-351 before phosphoenzyme conversion, differences between the spectra with the two isotopes will identify the absorbance of the phosphoenzyme phosphate group. As expected, the two spectra superimpose very well above 1250 cm^{-1}, where phosphate groups do not absorb. However, the band at 1192 cm^{-1} is reduced upon isotopic substitution. Instead, the intensity is higher for [γ-$^{18}O_3$]ATP between 1180 and 1150 cm^{-1}. A difference spectrum between labeled and unlabeled phosphate group (data not shown) shows that the band at 1192 cm^{-1} for the unlabeled phosphate seems to shift to 1157 cm^{-1} for the labeled phosphate, in agreement with the expected isotopic shift of 20–30 cm^{-1} for phosphate groups (18, 40). This identification of a phosphate band in the difference spectrum clearly shows that the conversion reaction considerably changes the environment of the phosphoenzyme phosphate group, thus affecting its electron density distribution and/or binding geometry. The band position at 1192 cm^{-1} is rather unusual for a phosphate group and could be explained in two ways: (i) a widening of the P–O angles leading to a stronger coupling between the P–O vibrations and thus to a stronger splitting between the ν_{as} and ν_s modes; or (ii) an increase in electron density of some or all of the P–O bonds, either by breaking of the hydrogen bonds to all phosphate oxygens or by strong hydrogen binding to one or two of the phosphate oxygen atoms, thus increasing the electron density in the other P–O bond(s). The band is also affected by $H_2O \rightarrow {}^2H_2O$ replacement, which seems to indicate that the phosphate oxygen interacts with either a water molecule or deuterated protein residues.

The active site of E_2-P was shown to be in a closed conformation (41) shielded from bulk water with a hydrophobic environment detected close to the ribose OH groups of a fluorescent ATP analogue (42, 43). This finding is in contrast to the properties of Ca_2E_1-P, and it is thought that the decrease in the

active site water activity upon the Ca_2E_1-P $\rightarrow E_2$-P conversion is responsible for the higher hydrolysis rate of E_2-P as compared with Ca_2E_1-P (44). The infrared spectra presented here show that this conformational change has a direct effect on phosphate conformation and/or electron density distribution. Creation of a hydrophobic environment alone however, may not be sufficient to explain the phosphate band at 1192 cm^{-1}, because dehydration of the model compound acetyl phosphate shifts the ν_{as} PO_3^{2-} band only from 1132 to 1177 cm^{-1} at most (data not shown).

Comparison with Spectra of ATPase Phosphorylation—Fig. 4 shows spectra in ^2H_2O of ATPase phosphorylation Ca_2E_1·ATP $\rightarrow$ Ca_2E_1-P (*solid line*) (21) and of the overall reaction of phosphorylation and phosphoenzyme conversion Ca_2E_1·ATP $\rightarrow$ E_2-P (*dotted line*). These spectra were obtained from time-resolved measurements of the same set of samples. Negative bands are characteristic for Ca_2E_1·ATP, positive bands either for Ca_2E_1-P (*solid line*) or E_2-P (*dotted line*). (The spectrum of Ca_2E_1·ATP $\rightarrow$ Ca_2E_1-P also shows a small contribution because of the E_2-P that is already formed, as indicated by the E_2-P marker band near 1750 cm^{-1}.) The spectral region shown includes the amide I region (1700–1610 cm^{-1}) that is sensitive to conformational changes of the protein backbone. The comparison indicates that bands characteristic for Ca_2E_1-P are still present in E_2-P, which is especially obvious for the bands at 1682, 1630, and 1593 cm^{-1}. This finding indicates that at least some of the alterations to the protein conformation induced by ATPase phosphorylation seem to be preserved or even "enhanced" in the subsequent transition to E_2-P. It seems as if the enzyme conformation on the way from Ca_2E_1-P to E_2-P goes further away from the pre-phosphorylation conformation of Ca_2E_1·ATP instead of returning to it.

CONCLUSIONS

Infrared difference spectra show that the protein conformation changes in the phosphoenzyme conversion reaction, preserving conformational changes of the preceding step of enzyme phosphorylation. β-sheet or turn structures of the extramembraneous domains and most likely α-helical structures seem to be affected. The net change of secondary structures, however, is small (10).

The release of Ca^{2+} proceeds from carboxylate groups that seem to be partly shielded from the aqueous environment. It is associated with the protonation of at least two carboxylate groups presumably involved in Ca^{2+} chelation. A change of environment of a Tyr residue was detected as well as a direct effect of phosphoenzyme conversion on the geometry and/or electron density distribution of the phosphoenzyme phosphate group. The latter is likely to be a prerequisite for the higher susceptibility toward hydrolytic attack of E_2-P as compared with Ca_2E_1-P. Interestingly, the currently assigned bands of the phosphate group and of Ca^{2+} release from carboxylate groups appear with the same reaction rate (10), showing that Ca^{2+} release and the change of phosphate environment proceed at the same time. This finding rules out a significant population of Ca_2E_2-P, a postulated state (45) with phosphate properties of E_2-P that still binds Ca^{2+}.

Acknowledgments—Valuable discussions with Prof. W. Mäntele and the opportunity to use his laboratory are gratefully acknowledged. The author thanks Prof. W. Hasselbach (Max-Planck-Institut, Heidelberg) for the gift of Ca^{2+}-ATPase, Dr. M. R. Webb (National Institute for Medical Research, London) for the gift of [γ-$^{18}O_3$]ATP, and Dr. J. E. T. Corrie (National Institute for Medical Research, London) for caging ATP and [γ-$^{18}O_3$]ATP.

REFERENCES

1. Andersen, J. P. (1989) *Biochim. Biophys. Acta* **988,** 47–72
2. Mintz, E., and Guillain, F. (1995) *Biosci. Rep.* **15,** 377–385
3. Inesi, G., Chen, L., Sumbilla, C., Lewis, D., and Kirtley, M. E. (1995) *Biosci. Rep.* **15,** 327–339
4. Andersen, J. P. (1995) *Biosci. Rep.* **15,** 243–261
5. Mintz, E., and Guillain, F. (1997) *Biochim. Biophys. Acta* **1318,** 52–70
6. Barth, A., Mäntele, W., and Kreutz, W. (1991) *Biochim. Biophys. Acta* **1057,** 115–123
7. Barth, A., Mäntele, W., and Kreutz, W. (1990) *FEBS Lett.* **277,** 147–150
8. Barth, A., Kreutz, W., and Mäntele, W. (1994) *Biochim. Biophys. Acta* **1194,** 75–91
9. Georg, H., Barth, A., Kreutz, W., Siebert, F., and Mäntele, W. (1994) *Biochim. Biophys. Acta* **1188,** 139–150
10. Barth, A., von Germar, F., Kreutz, W., and Mäntele, W. (1996) *J. Biol. Chem.* **271,** 30637–30646
11. Troullier, A., Gerwert, K., and Dupont, Y. (1996) *Biophys. J.* **71,** 2970–2983
12. Buchet, R., Jona, I., and Martonosi, A. (1991) *Biochim. Biophys. Acta* **1069,** 209–217
13. Buchet, R., Jona, I., and Martonosi, A. (1992) *Biochim. Biophys. Acta* **1104,** 207–214
14. McCray, J. A., and Trentham, D. R. (1989) *Annu. Rev. Biophys. Biophys. Chem.* **18,** 239–270
15. Corrie, J. E. T., and Trentham, D. R. (1993) in *Bioorganic Photochemistry* (Morrison, H., ed) Vol. 2, pp. 243–305, John Wiley & Sons, New York
16. Adams, S. R., and Tsien, R. Y. (1993) *Annu. Rev. Physiol.* **55,** 755–783
17. Kaplan, J. H. (1990) *Annu. Rev. Physiol.* **52,** 897–914
18. Barth, A., Hauser, K., Mäntele, W., Corrie, J. E. T., and Trentham, D. R. (1995) *J. Am. Chem. Soc.* **117,** 10311–10316
19. Barth, A., Corrie, J. E. T., Gradwell, M. J., Maeda, Y., Mäntele, W., Meier, T., and Trentham, D. R. (1997) *J. Am. Chem. Soc.* **119,** 4149–4159
20. Cepus, V., Ulbrich, C., Allin, C., Troullier, A., and Gerwert, K. (1998) *Methods Enzymol.* **291,** 223–245
21. Barth, A., and Mäntele, W. (1998) *Biophys. J.* **75,** 538–544
22. Sawyer, D. T., and Tackett, J. E. (1963) *J. Am. Chem. Soc.* **85,** 314–316
23. Nakamoto, K., Morimoto, Y., and Martell, A. E. (1963) *J. Am. Chem. Soc.* **85,** 309–313
24. Tackett, J. E. (1989) *Appl. Spectrosc.* **43,** 483–489
25. Venyaminov, S. Y., and Kalnin, N. N. (1990) *Biopolymers* **30,** 1243–1257
26. Chirgadze, Y. N., Fedorov, O. V., and Trushina, N. P. (1975) *Biopolymers* **14,** 679–694
27. Byler, D. M., and Susi, H. (1986) *Biopolymers* **25,** 469–487
28. Susi, H., Timasheff, N., and Stevens, L. (1967) *J. Biol. Chem.* **242,** 5460–5466
29. Haris, P. I., and Chapman, D. (1994) in *Methods in Molecular Biology, Microscopy, Optical Spectroscopy, and Macroscopic Techniques.* (Jones, C., Mulloy, B., and Thomas, A. H., eds) Vol. 22, pp. 183–202, Humana Press, Totowa, NJ
30. Hienerwadel, R., Boussac, A., Breton, J., Diner, B., and Berthomieu, C. (1997) *Biochemistry* **36,** 14712–14723
31. Pinchas, S., and Laulicht, I. (1971) *Infrared Spectra of Labelled Compounds*, pp. 133–136, Academic Press, London
32. Deacon, G. B., and Phillips, R. J. (1980) *Coord. Chem. Rev.* **33,** 227–250
33. Barth, A., Mäntele, W., and Kreutz, W. (1997) *J. Biol. Chem.* **272,** 25507–25510
34. Green, N. M., Taylor, W. R., Brandl, C. J., Korczak, B., and MacLennan, D. H. (1986) *CIBA Found. Symp.* **122,** 93–114
35. Brandl, C. J., Green, N. M., Korczak, B., and MacLennan, D. H. (1986) *Cell* **44,** 597–607
36. Doyle, B. B., Traub, W., Lorenzi, G. P., and Blout, E. R. (1971) *Biochemistry* **10,** 3052–3061
37. Goormaghtigh, E., Cabiaux, V., and Ruysschaert, J.-M. (1994) in *Subcellular Biochemistry* (Hilderson, H. J., and Ralston, G. B., eds) pp. 329–362, Plenum Press, New York
38. Lautié, A., Lautié, M. F., Gruger, A., and Fakhri, S. A. (1980) *Spectrochim. Acta Part A Mol. Spectrosc.* **36,** 85–94
39. Takeuchi, H., and Harada, I. (1986) *Spectrochim. Acta Part A Mol. Spectrosc.* **42,** 1069–1078
40. Takeuchi, H., Murata, H., and Harada, I. (1988) *J. Am. Chem. Soc.* **110,** 392–397
41. Highsmith, S. (1986) *Biochemistry* **25,** 1049–1054
42. Dupont, Y., and Pougeois, R. (1983) *FEBS Lett.* **156,** 93–98
43. Nakamoto, R. K., and Inesi, G. (1984) *J. Biol. Chem.* **259,** 2961–2970
44. De Meis, L., and Suzano, V. A. (1988) *FEBS Lett.* **232,** 73–77
45. Inesi, G., and De Meis, L. (1985) in *The Enzymes of Biological Membranes* (Martonosi, A., ed) 2nd Ed., Vol. 3, pp. 157–191, Plenum Press, New York